Talanta 134 (2015) 54–59

Contents lists available at ScienceDirect

Talanta

journal homepage: www.elsevier.com/locate/talanta

One-pot synthesis of gold nanoclusters with bright red fluorescence and good biorecognition Abilities for visualization fluorescence enhancement detection of *E. coli*

Jiali Liu, Lili Lu, Suying Xu*, Leyu Wang*

State Key Laboratory of Chemical Resource Engineering, Beijing Key Laboratory of Environmentally Harmful Chemical Analysis, Beijing University of Chemical Technology, Beijing 100029, P.R. China

ARTICLE INFO

Article history:
Received 18 August 2014
Received in revised form
22 October 2014
Accepted 28 October 2014
Available online 6 November 2014

Keywords:
Lysozyme
Gold nanoclusters
Bacteria
Fluorescence enhancement detection

ABSTRACT

A facile one-pot strategy was developed for the synthesis of lysozyme functionalized fluorescence gold nanoclusters (AuNCs). The lysozymes added to reduce Au^{3+} ions and stabilize the AuNCs during the synthesis were coated on the AuNCs surface and retained their specific recognition ability for bacteria such as Escherichia coli (*E. coli*). Based on such ability, these AuNCs were specifically attached onto the surface of *E. coli*, which resulted in great red fluorescence enhancement. Nevertheless, the bovine serum albumin (BSA) stabilized AuNCs could not recognize *E. coli* and no fluorescence enhancement was observed. Upon the addition of *E. coli*, the red fluorescence intensity of lysozyme-AuNCs was enhanced linearly over the range of $2.4 \times 10^4 - 6.0 \times 10^6$ CFU/mL of *E. coli* with high sensitivity (LOD$=2.0 \times 10^4$ CFU/mL, S/N$=3$). The visualization fluorescence evolution may enable the rapid and real-time detection of bacteria. This study may be extended to other functional proteins such as antibody, enzyme, and peptide functionalized nanoclusters while retaining the bioactivity of coating proteins and find wide applications in the fields of biochemistry and biomedicine.

1. Introduction

Bacterial infection caused by pathogen bacteria is a major threat to human health (e.g. *Escherichia coli*) due to their easy survival and spread in the challenging environment. Treatments for bacterial infection often involve cost. The rapid and sensitive detection of bacteria for public health, food safety, timely disease diagnosis and treatment is highly desirable. The conventional techniques of identification and quantitative detection of bacteria mainly rely on culture and colony counting of bacteria. In recent years, a variety of methods have been developed, such as enzyme-linked immunosorbent assays (ELISAs), chemiluminescence, electrochemistry, and fluorescence spectroscopy. [1–8] However, these methods are confined to laboratory and complicated that pose a challenge to the rapid and practical detection of bacteria.

The unique physicochemical, optical, and electrical properties of nanomaterials [9–19] including noble metal nanoclusters (NCs) have stimulated great interests for their applications in biological imaging, [20,21] catalysis [9,22], and chemical sensors [18,23–26]. Among the various noble metal clusters reported to date, gold nanoclusters (AuNCs) are the prominent member due to their relatively easy preparation, ultrafine size, bright fluorescence, high solubility, biocompatibility, low toxicity, and high stability in ambient conditions. In order to prepare non-cytotoxic and multifunctional fluorescent AuNCs, various methods using biocompatible reducing or stabilizing agents, such as proteins and peptides, have been developed as the thiol, amine, and carboxyl groups in proteins have high affinities for gold ions and reducing groups (phenol and thiol groups) in proteins reduce the gold ions to atoms. [27–30] Thus proteins have played an essential part in the synthesis of fluorescent AuNCs, considering their size control ability and the mild reaction conditions. [31] Up to now, several proteins, such as bovine serum albumin (BSA), [27,32] insulin, [33] horseradish peroxidase, [28] pepsin, [34] lactotransferrin, [35] as well as lysozyme [36,37] have been employed as templates for the preparation of the fluorescent AuNCs. In order get the strong fluorescence, these NCs were generally synthesized at high pH and relatively high temperature, which would result in the loss of protein bioactivity although the NCs were stabilized by coating proteins. In most cases, it is necessary to further label the protein stabilized NCs with antibodies before the fluorescence immunoassay and imaging applications. Therefore, it is still a challenge to develop a facile one-pot strategy to synthesize the enzyme functionalized AuNCs with strong fluorescence and good stability while retaining the enzyme bioactivity.

*: Corresponding authors.
E-mail addresses: kkxsy@163.com (S. Xu), lywang@mail.buct.edu.cn (L. Wang).

http://dx.doi.org/10.1016/j.talanta.2014.10.058
0039-9140/

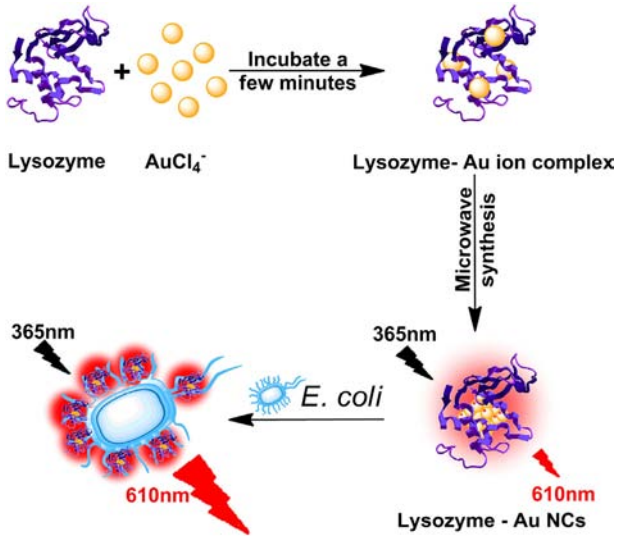

Scheme 1. Schematic diagram of the synthesis of the red fluorescent lysozyme-Au NCs and fluorescence enhancement detection of *E. coli*.

Herein, we developed a facile one-pot, microwave-assisted strategy for the synthesis of fluorescent AuNCs by using lysozyme as a template (Scheme 1). We choose lysozyme as the stabilizer owing to the unique properties of the lysozeme: a) Lysozyme (pI = 11.3) is a alkaline protein consisting of 129 amino acid residues with abundant free carboxylic groups, amino groups and four disulfide bonds, which is suitable for the gold ion reduction and AuNCs stabilization. [38,39] b) Lysozyme is highly stable and its bioactivity is well retained even treated over 90 °C for 15 min, which is highly desirable for fluorescent AuNCs with specific bio-recognition ability. [40]c) Lysozyme is a family of enzymes that can recognize and kill bacteria. [41] Therefore, the lysozyme functionalized fluorescence AuNCs would be used directly for the bacterium detection. As shown in Scheme 1, owing to the specific recognition between lysozymes and *E. coli*, the fluorescent lysozyme-AuNCs were attached onto the surface of *E. coli*. Consequently, the red fluorescence was greatly and linearly enhanced over the range of $2.4 \times 10^4 - 6.0 \times 10^6$ CFU/mL of *E. coli* and a fluorescence enhancement nanobiosensor for *E. coli* was successfully designed. Moreover, the bacteria coated with AuNCs were precipitated at the bottom of the vial through centrifugation, and the fluorescence of supernatants was obviously decreased, and thus a fluorescence visualization assay method for *E. coli* was proposed. The conventional techniques of identification and quantitative detection of bacteria methods (culture and colony counting of bacteria) have several drawbacks such as low sensitivity, time-consuming and complicated operation procedures. Though some of the reported examples [42–44] showed the good capability for *E. coli* recognition, yet either toxic materials were involved or unsatisfactory performance (limits of detection in the range of $10^3 - 10^4$ CFU/mL) were observed. The method we proposed exhibited a good linearity range and low detection limit as well as having the advantages of rapid, real-time and easy operation.

2. Experiment section

2.1. Chemicals and materials

Lysozyme (CAS number: 12650-88-3, E.C. number: 235–747-3) from chicken egg white was purchased from NOVON. Hydrogen tetrachloroaurate (III) tetrahydrate ($HAuCl_4 \cdot 4H_2O$) and trihydroxymethyl aminomethane-hydrochloric acid (Tris–HCl) were obtained from Sinopharm Chemical Reagent Co., Ltd. Sodium hydroxide (NaOH), acetic acid (CH_3COOH), sodium acetate (CH_3COONa), sodium carbonate (Na_2CO_3), sodium bicarbonate ($NaHCO_3$), citric acid ($C_6H_8O_7 \cdot H_2O$), ethanol, and ascorbic acid (vitamin C) were acquired from Beijing Chemical Factory. L-cysteine (Cys) and L-tyrosine (Tyr) were purchased from Beijing AOBOX Biotechnology Co., Ltd. Sodium borohydride ($NaBH_4$) was purchased from Tianjin Fuchen Chemical Reagents Factory. *Escherichia coli DH5α* was provided by Tiangen Biotech (Beijing) Co., Ltd. Luria-Bertani broth (LB broth) and kanamycin sulfate (KANA) were obtained from Beijing Solarbio Science & Technology Co., Ltd. All the chemicals were of analytical grade and used as received without further purification. Ultrapure water was used throughout and prepared by MillïQ water (Millipore Co., Bedford, MA).

2.2. Characterization

The shape and size of the lysozyme-gold nanoclusters (AuNCs) were examined through a JEOL JEM-1200EX transmission electron microscope (TEM) with a tungsten filament at an accelerating voltage of 100 kV. Dynamic light scattering (DLS) particle size analysis of aqueous lysozyme-Au NCs was carried out on a Zetasizer Nano-ZS90 (Malvern) zeta and size analyzer. The fluorescence spectra of the lysozyme-AuNCs were measured through a Hitachi F-4600 fluorescence spectrophotometer equipped with a plotter unit and a quartz cell (1 cm × 1 cm).

2.3. Synthesis of the red fluorescent lysozyme-AuNCs

All glasswares used here were washed with Aqua Regia (HCl:HNO_3 volume ratio = 3:1), and rinsed with sodium hydroxide solution and ultrapure water. (Caution: Aqua Regia is a very corrosive oxidizing agent, which should be handled with great care.) The lysozyme stabilized gold nanoclusters were prepared through microwave-assisted synthesis method. Because the lysozyme was easily inactivated in the alkaline environment, we decided to synthesize the lysozyme-Au NCs in neutral or weak acid conditions (pH 6.0). But the Au^{3+} wouldn't be reduced into AuNCs under this pH range, so we add an additional reductant, L-cysteine, to assist this reaction. To examine the influence of different experiment conditions on the synthesis of lysozyme-AuNCs, we investigated the reaction temperature, the reaction time, the pH values of reaction mixture solution, the amount of the reactant, and the mole ratio of lysozyme, $HAuCl_4$, and L-cysteine. Under an optimal condition, aqueous $HAuCl_4$ solution (10 mM, 0.5 mL) was added to the lysozyme solution (10 mg/mL, 0.5 mL) under vigorous stirring. 8.5 mL of ultrapure water and 0.5 mL of L-cysteine solution (10 mM) were introduced a few minutes later. Subsequently, the solution pH was adjusted to ~6.0 by adding aqueous sodium hydroxide (1 M, 15 μL). The mixture solution was vigorously stirred for another 10 min at room temperature. The resulting mixture solution was then placed in a single mode microwave synthesizer (NOVA-2 S, produced by PreeKem Scientific Instruments Co.,Ltd.) to proceed under vigorous stirring at 90 °C for 10 min or at 70 °C for 15 min. The mixture was then allowed to cool to room temperature before the centrifugation at 9000 rpm (rotor radius: 8.5 cm) for 10 min to remove the large size gold nanoparticles (Au NPs).

2.4. Preparation of bacteria

E. coli were cultured in LB broth (5 mL) including KANA (which was prepared by dissolving 0.125 g of LB broth, 25 μg KANA in 5 mL of deionized water). After incubation for 12 ~ 16 h at 37 °C in the incubator (180 rpm/min), the bacterial cells were then isolated through centrifugation (9000 rpm/min, 10 min). The bacterial cell suspension was re-dissolved in a proper solution for later use.

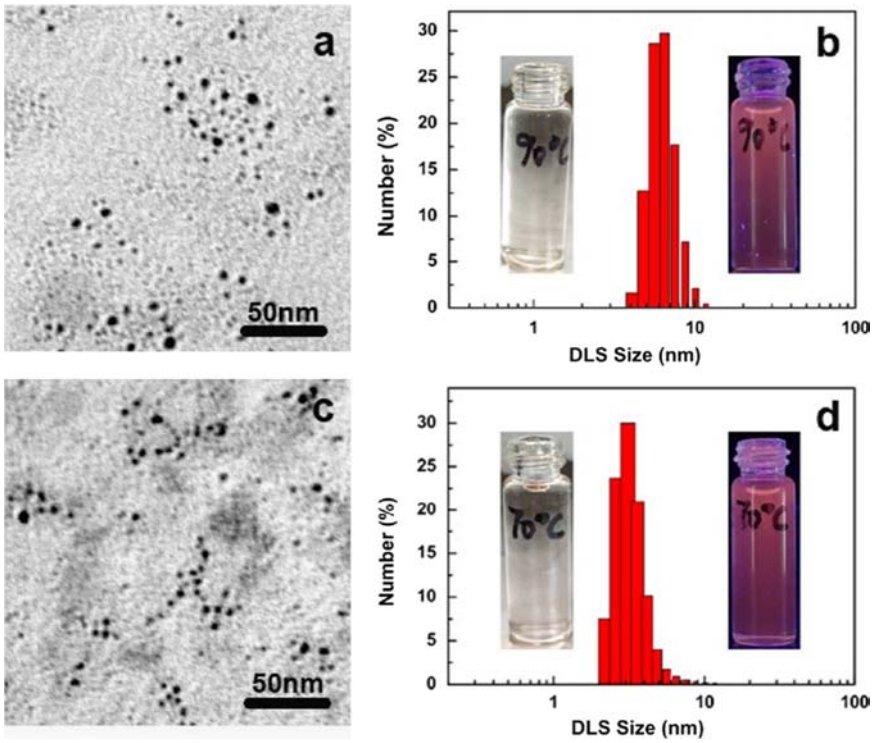

Fig. 1. TEM images (a and c) and DLS size distribution profiles (b and d) of the lysozyme-AuNCs prepared at 90 °C for 10 min (a and b) and 70 °C for 15 min (c and d), respectively. Insets: the optical photos of lysozyme-AuNCs dispersed in ultrapure water under natural light (left) and 365 – nm UV light. The concentration of the lysozyme-AuNCs colloidal solution is 0.5 mM.

2.5. Fluorescence turn-on detection of E. coli

In brief, in a 1.5 – mL vial, 100.0 μL of the lysozyme-AuNCs solution (0.5 mM) was mixed with various concentrations of *E. coli*, and then the mixed solution was diluted to 1.0 mL with Tric-HCl buffer solution (pH 6.0, 20.0 mM) before mixing the solution thoroughly. Then the Fluorescence spectra of the mixture solution were carried out under UV light irradiation (365 nm).

3. Results and discussion

3.1. Characterization of lysozyme-AuNCs

The shape and size of the lysozyme-AuNCs were examined through transmission electron microscope (TEM) and dynamic light scattering (DLS) technology. From the TEM images and DLS size distribution profiles shown in Fig. 1, it can be seen that the as-prepared lysozyme-AuNCs are small NCs with an average size around 3 – 6 nm. The size distribution of lysozyme-AuNCs synthesized at 90 °C for 10 min is somewhat wider than that of synthesized at 70 °C for 15 min. Due to the good water-solubility of lysozyme, the lysozyme-AuNCs can be well dispersed in kinds of aqueous solutions, such as $CH_3COOH-CH_3COONa$, Tris – HCl, and $Na_2CO_3-NaHCO_3$ buffer solution. As shown in the insets of Fig. 1b and d, the lysozyme-AuNCs are well dispersed in ultrapure water. Under the excitation of 365 – nm UV light, these lysozyme-AuNCs demonstrate relatively strong red fluorescence. Although these lysozyme-AuNCs are synthesized under different conditions, their fluorescence brightness has no obvious difference. Since some gold nanoparticles without fluorescence were also observed when being synthesized at 90 °C. Therefore, we prepared the lysozyme-AuNCs for later use by treating the mixture reaction solution at 70 °C for 15 min. The as-prepared lysozyme-AuNCs seem very stable since bright red fluorescence still could be observed though stored at 4 °C for at least three months.

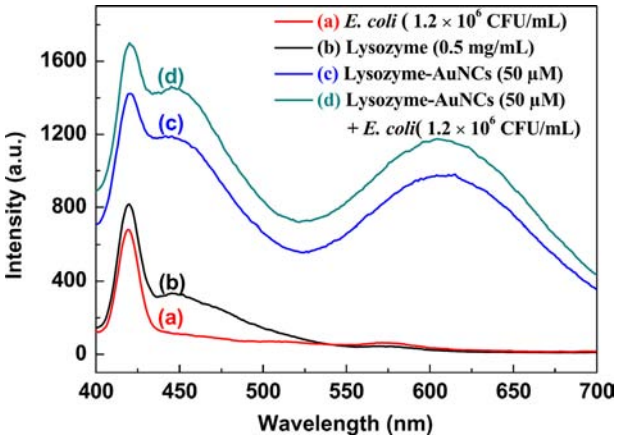

Fig. 2. Fluorescence spectra of lysozyme (a), *E. coli* (b), lysozyme-AuNCs (c), and lysozyme-AuNCs + *E.coli* (d).

To demonstrate their applications for bacterium recognition, the fluorescence spectra of these NCs were further investigated. As shown in Fig. 2, under the 365 – nm light irradiation, both the lysozyme (Fig. 2a) and *E. coli* (Fig. 2b) demonstrate strong fluorescence in the range of 400 – 500 nm resulted from proteins, but no red fluorescence can be observed. In the spectrum of lysozyme-AuNCs, a red emission peak centered at 610 nm was observed besides the fluorescence of proteins (Fig. 2c). With the addition of *E. coli*, the red fluorescence was dramatically enhanced (Fig. 2d). All the results indicate that the red fluorescence resulted from the gold nanoclusters, and these lysozyme-AuNCs are suitable for fluorescence enhancement detection of bacteria.

3.2. Fluorescence visualization detection of E. coli

To test the possibility and explore the mechanism for the fluorescence enhancement detection of *E. coli* by using the

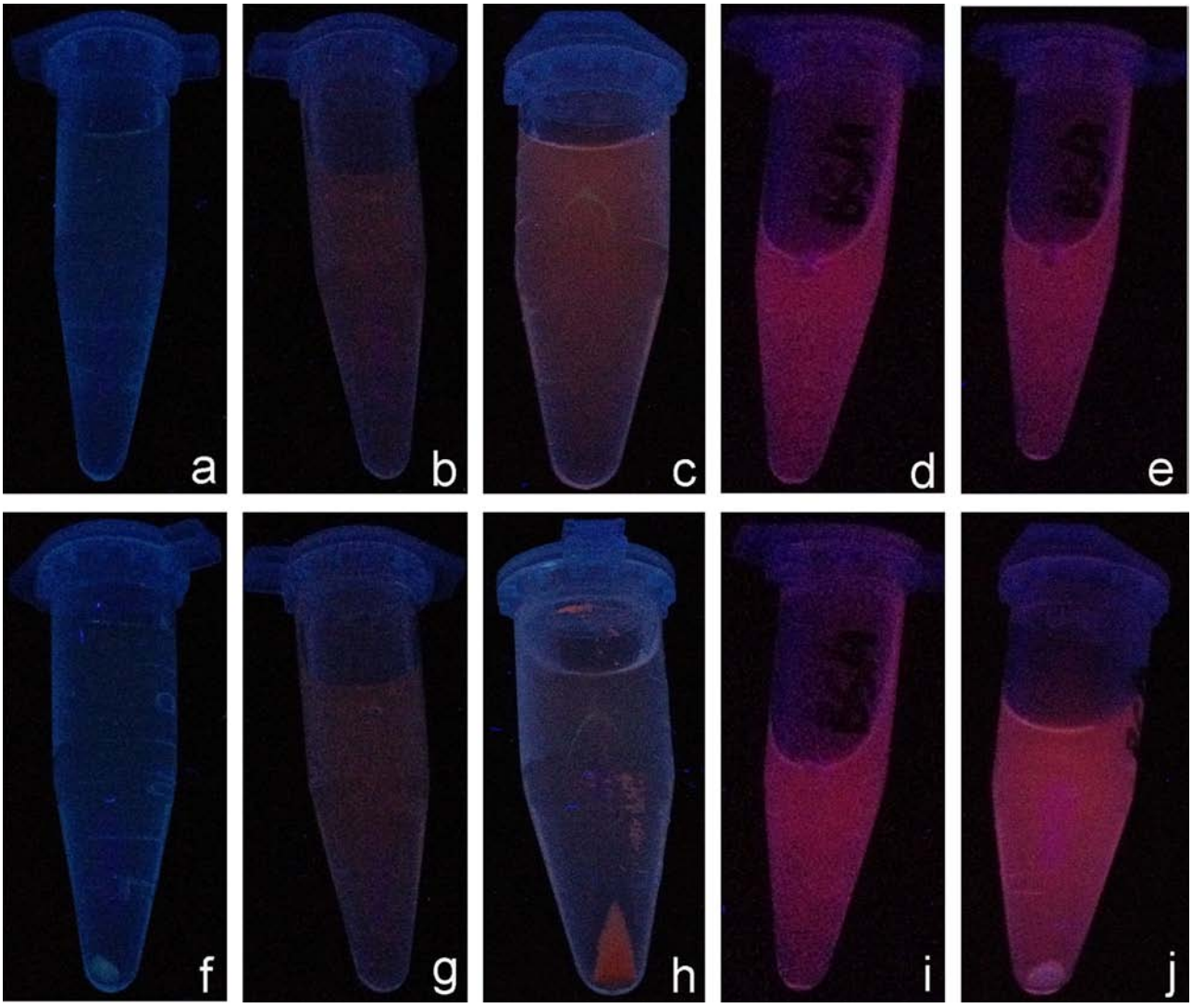

Fig. 3. Optical photos of *E. coli* (a and f), lysozyme-AuNCs (b and g), lysozyme-AuNCs+*E. coli* (c and h), BSA-AuNCs (d and i) and BSA-AuNCs+*E. coli* (e and j) before (a–e) and after (f–j) centrifugation. Excitation: 365 nm. NCs: 0.25 mM. *E. coli*: 1.5×10^7 CFU/mL.

lysozyme-AuNCs, the optical behaviors of the AuNCs under various conditions were carried out. Fig. 3 presented the optical photos of *E. coli* (Fig. 3a and f), lysozyme-AuNCs (Fig. 3b and g), lysozyme-Au NCs+*E. coli* (Fig. 3c and h), bovine serum albumin (BSA)-AuNCs (Fig. 3d and i) and BSA- AuNCs+*E. coli* (Fig. 3e and j) before (a–e) and after (f–j) centrifugation at 9000 rpm. As shown in Fig. 3a and f, no red fluorescence was observed from the *E. coli* solution. After the centrifugation, all the *E. coli* have been precipitated at the bottom of the vial (Fig. 3h and j). However, for the lysozyme-AuNCs, because they are unable to be precipitated at this centrifugation speed, we cannot see any bright spots of the lysozyme-AuNCs at the bottom (Fig. 3b and g). Once the lysozyme-AuNCs attached to the target bacteria, the lysozyme-AuNCs go down with the bacteria even under a low centrifugation speed (Fig. 3c and h). Compared to Fig. 3b, the addition of *E. coli* dramatically enhanced the red fluorescence (Fig. 3c). Nevertheless, after the centrifugation, all the red fluorescent NCs were dropped along with the *E. coli* down to the bottom of the vial, and no red fluorescence was observed in the supernatants (Fig. 3h). As a control, the red fluorescence of BSA-AuNCs was not influenced by the addition of *E. coli*, indicating the specific binding of lysozyme toward *E. coli*. After the centrifugation, only white *E. coli* but not red fluorescent BSA-AuNCs were spun down at the bottom of the vial (Fig. 3j). Apparently, these results indicate that the bioactivity of lysozyme on the lysozyme-AuNCs is well retained and these NCs can be used for fluorescence enhancement detection of *E. coli*.

3.3. Influence of pH

To construct the lysozyme-AuNCs nanosensor for bacteria detection, the influence of pH values on the fluorescence intensity was also studied over a wide pH range of 3.0–11.0. As depicted in Fig. 4, the fluorescence intensity of lysozyme-AuNCs showed a strong dependent of the pH values. When the pH value is over 10, the fluorescence intensity was dramatically quenched. To the best of our knowledge, lysozyme can be inactive under alkaline conditions. We proposed that the structure of lysozyme-AuNCs may be destroyed, which results in the aggregation of AuNCs and thus fluorescence quenching. Under the mildly acidic conditions, the addition of *E. coli* caused a strong and steady fluorescence enhancement. Taking the lysozyme activity into consideration, the pH 6.0 was chosen as the optimal pH condition, because under this pH the activity of the lysozyme is well retained.

3.4. Fluorescence evolution of lysozyme-AuNCs towards E. coli concentration

Under the optimal conditions, we studied the fluorescence evolution of the lysozyme-AuNCs versus *E. coli* concentrations in the range

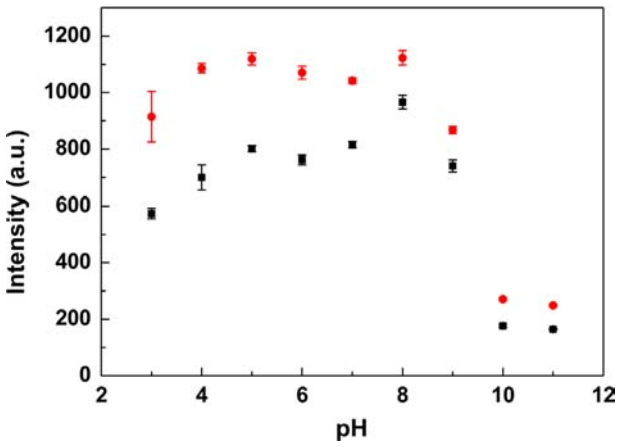

Fig. 4. pH effect on the fluorescence intensity of lysozyme-AuNCs in the absence (black and square dot) and presence (red and round dot) of *E. coli*. Buffer solution: pH (3, 4): $CH_3COOH-CH_3COONa$ (20.0 mM); pH (6–9): Tris–HCl (20.0 mM); pH (10–11): $Na_2CO_3-NaHCO_3$ (20.0 mM). $\lambda_{ex}/\lambda_{em}$=365 nm/610 nm. Lysozyme-AuNCs: 50.0 μM; *E. coli*: 4.7 × 10^6 CFU/mL.

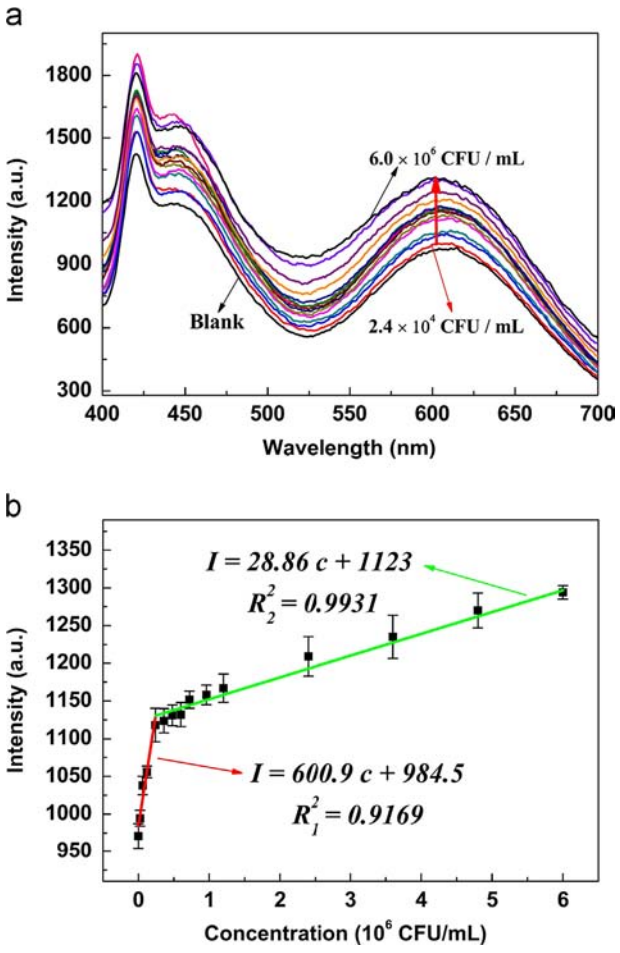

Fig. 5. (a) Evolution of red fluorescence spectra of lysozyme-AuNCs vs *E. coli* concentrations. (b) The calibration plots of red fluorescence intensity vs *E. coli* concentrations, $\lambda_{ex}/\lambda_{em}$=365 nm/610 nm. Lysozyme-AuNCs: 50.0 μM; Buffer solution: Tris–HCl (pH 6.0, 20.0 mM).

of 2.4 × 10^4 –6.0 × 10^6 CFU/mL. In brief, the *E. coli* sample solution was mixed with the Tris–HCl buffer solution (pH 6.0, 20.0 mM) containing 100 μL of the as-prepared lysozyme-AuNCs (0.5 mM), and was then incubated at room temperature for 5 min before recording the fluorescence spectrum. As shown in Fig. 5, the red fluorescence intensity of lysozyme-AuNCs was enhanced linearly along with the increased concentration of *E. coli* over the range of 2.4 × 10^4 –6.0 × 10^6 CFU/mL. The limit of detection (LOD=3σ/K) for *E. coli* was 2.0 × 10^4 CFU/mL. Herein, σ is the standard deviation of the blank measurements (n=6) and *K* is the slope of the calibration curve. In addition, the first calibration function for the *E. coli* analysis from 2.4 × 10^4 –2.4 × 10^5 CFU/mL is $I=600.9\,C\ (\times 10^6\ CFU/mL)+984.5$ (n=5, which means there are five experimental data on the linear plot) with a good linearity (R_1^2=0.9169). The second calibration function for the *E. coli* analysis from 2.4 × 10^5 –6.0 × 10^6 CFU/mL is $I=28.86\,C\ (\times 10^6\ CFU/mL)+1123$ (n=11, R_2^2=0.9931). Herein, *I* is the fluorescence intensity of the lysozyme-AuNCs and *C* is the mass concentration of *E. coli* ($\times 10^6$ CFU/mL). These results suggest that our red fluorescence lysozyme-AuNCs are applicable for the fluorescence enhancement detection of *E. coli* in a wide concentration range.

4. Conclusion

In conclusion, we developed a green and facile one-pot microwave-assisted method for the synthesis of red fluorescence gold nanoclusters (AuNCs) using lysozyme as a template, in which the lysozyme activity is well retained. Based on the specific recognition between the lysozyme and bacteria, these lysozyme functionalized AuNCs have been successfully designed for the fluorescence enhancement detection of *E. coli* over the range of 2.4 × 10^4 –6.0 × 10^6 CFU/mL with high a sensitivity (LOD=2.0 × 10^4 CFU/mL). The visualization fluorescence evolution may enable the rapid and real-time detection of bacteria. These unique features of the lysozyme-AuNCs may allow their applications in the biomedical and biological fields in the future. This method has the potential to be further extended to other types of protein protected metal NCs while retaining good bioactivities.

Notes

The authors declare no competing financial interest.

Acknowledgments

This research was supported in part by the National Natural Science Foundation of China (21475007 and 21275015), the State Key Project of Fundamental Research of China (2011CB932403 and 2011CBA00503), the Fundamental Research Funds for the Central Universities (ZZ1321 and YS1406), the Scientific Research Foundation for the Returned Overseas Chinese Scholars, State Education Ministry, and the Program for Changjiang Scholars and Innovative Research Team in University (IRT1205). We also thank the support from the "Public Hatching Platform for Recruited Talents of Beijing University of Chemical Technology".

References

[1] K. Knez, K.P.F. Janssen, D. Spasic, P. Declerck, L. Vanysacker, C. Denis, D.T. Tran, J. Lammertyn, Anal. Chem. 85 (2013) 1734–1742.
[2] Y.V. Gerasimova, D.M. Kolpashchikov, Angew. Chem. Int. Edit 52 (2013) 10586–10588.
[3] O.R. Miranda, X.N. Li, L. Garcia-Gonzalez, Z.J. Zhu, B. Yan, U.H.F. Bunz, V.M. Rotello, J. Am. Chem. Soc. 133 (2011) 9650–9653.
[4] X.F. Guo, A. Kulkarni, A. Doepke, H.B. Halsall, S. Iyer, W.R. Heineman, Anal. Chem. 84 (2012) 241–246.
[5] C. Tlili, E. Sokullu, M. Safavieh, M. Tolba, M.U. Ahmed, M. Zourob, Anal. Chem. 85 (2013) 4893–4901.
[6] S.J. Wu, N. Duan, Z. Shi, C.C. Fang, Z.P. Wang, Anal. Chem. 86 (2014) 3100–3107.
[7] Y. Zhag, C. Tan, R.H. Fei, X.X. Liu, Y. Zhou, J. Chen, H.C. Chen, R. Zhou, Y.G. Hu, Anal. Chem. 86 (2014) 1115–1122.
[8] R. Mukherji, A. Samanta, R. Illathvalappil, S. Chowdhury, A. Prabhune, R.N. Devi, ACS. Appl. Mater. Interfac. 5 (2013) 13076–13081.

[9] D. Liu, B.Q. Lin, W. Shao, Z. Zhu, T.H. Ji, C.Y. Yang, ACS. Appl. Mater. Interfac. 6 (2014) 2131–2136.
[10] X. Lin, L. Cui, Y. Huang, Y. Lin, Y. Xie, Z. Zhu, B. Yin, X. Chen, C.J. Yang, Chem. Commun. 50 (2014) 7646–7648.
[11] Q. Liu, J.J. Peng, L.N. Sun, F.Y. Li, ACS. Nano 5 (2011) 8040–8048.
[12] L.Q. Xiong, Z.G. Chen, Q.W. Tian, T.Y. Cao, C.J. Xu, F.Y. Li, Anal. Chem. 81 (2009) 8687–8694.
[13] K. Zhang, H.B. Zhou, Q.S. Mei, S.H. Wang, G.J. Guan, R.Y. Liu, J. Zhang, Z.P. Zhang, J. Am. Chem. Soc. 133 (2011) 8424–8427.
[14] P.P. Wang, Y. Yang, J. Zhuang, X. Wang, J. Am. Chem. Soc. 135 (2013) 6834–6837.
[15] Z.C. Zhang, Y.F. Chen, X.B. Xu, J.C. Zhang, G.L. Xiang, W. He, X. Wang, Angew. Chem. Int. Edit 53 (2014) 429–433.
[16] H. Pei, X.L. Zuo, D. Zhu, Q. Huang, C.H. Fan, Accounts Chem. Res. 47 (2014) 550–559.
[17] D.G. Wang, Y.Y. Zhang, J.Q. Wang, C. Peng, Q. Huang, S. Su, L.H. Wang, W. Huang, C.H. Fan, ACS. Appl. Mater. Interfac. 6 (2014) 36–40.
[18] N.N. Tu, L.Y. Wang, Chem. Commun. 49 (2013) 6319–6321.
[19] Y.X. Ma, H. Li, S. Peng, L.Y. Wang, Anal. Chem. 84 (2012) 8415–8421.
[20] C.L. Liu, H.T. Wu, Y.H. Hsiao, C.W. Lai, C.W. Shih, Y.K. Peng, K.C. Tang, H.W. Chang, Y.C. Chien, J.K. Hsiao, J.T. Cheng, P.T. Chou, Angew. Chem. Int. Edit 50 (2011) 7056–7060.
[21] Y. Tao, Z.H. Li, E.G. Ju, J.S. Ren, X.G. Qu, Nanoscale 5 (2013) 6154–6160.
[22] M. Liang, L.B. Wang, X. Liu, W. Qi, R.X. Su, R.L. Huang, Y.J. Yu, Z.M. He, Nanotechnology 24 (2013) 245601.
[23] Y. Yue, T.Y. Liu, H.W. Li, Z.Y. Liu, Y.Q. Wu, Nanoscale 4 (2012) 2251–2254.
[24] R. Ghosh, A.K. Sahoo, S.S. Ghosh, A. Paul, A. Chattopadhyay, ACS. Appl. Mater. Interfac. 6 (2014) 3822–3828.
[25] H. Li, L.Y. Wang, ACS. Appl. Mater. Interfac. 5 (2013) 10502–10509.
[26] Y.Y. Zhao, Y.X. Ma, H. Li, L.Y. Wang, Anal. Chem. 84 (2012) 386–395.
[27] J.P. Xie, Y.G. Zheng, J.Y. Ying, J. Am. Chem. Soc. 131 (2009) 888–889.
[28] F. Wen, Y.H. Dong, L. Feng, S. Wang, S.C. Zhang, X.R. Zhang, Anal. Chem. 83 (2011) 1193–1196.
[29] Q. Wen, Y. Gu, L.J. Tang, R.Q. Yu, J.H. Jiang, Anal. Chem. 85 (2013) 11681–11685.
[30] X. Le Guevel, N. Daum, M. Schneider, Nanotechnology 22 (2011) 275103.
[31] Y.L. Xu, J. Sherwood, Y. Qin, D. Crowley, M. Bonizzoni, Y.P. Bao, Nanoscale 6 (2014) 1515–1524.
[32] Y.C. Wang, Y. Wang, F.B. Zhou, P. Kim, Y.N. Xia, Small 8 (2012) 3769–3773.
[33] Y.H. Lin, W.L. Tseng, Anal. Chem. 82 (2010) 9194–9200.
[34] H. Kawasaki, K. Hamaguchi, I. Osaka, R. Arakawa, Adv. Funct. Mater. 21 (2011) 3508–3515.
[35] P.L. Xavier, K. Chaudhari, P.K. Verma, S.K. Pal, T. Pradeep, Nanoscale 2 (2010) 2769–2776.
[36] J. Das, S.O. Kelley, Anal. Chem. 85 (2013) 7333–7338.
[37] W.Y. Chen, J.Y. Lin, W.J. Chen, L.Y. Luo, E.W.G. Diau, Y.C. Chen, Nanomedicine 5 (2010) 755–764.
[38] C.C. Blake, D.F. Koenig, G.A. Mair, A.C. North, D.C. Phillips, V.R. Sarma, Nature 206 (1965) 757–761.
[39] L.N. Johnson, D.C. Phillips, Nature 206 (1965) 761–763.
[40] T. Masuda, Y. Ueno, N. Kitabatake, J. Agric. Food Chem. 49 (2001) 4937–4941.
[41] D.J. Vocadlo, G.J. Davies, R. Laine, S.G. Withers, Nature 412 (2001) 835–838.
[42] V. Duplan, E. Frost, J.J. Dubowski, Sens. Actuat. B-Chem. 160 (2011) 46–51.
[43] X.H. Xue, J. Pan, H.M. Xie, J.H. Wang, S. Zhang, Talanta 77 (2009) 1808–1813.
[44] L.J. Yang, Y.B. Li, Analyst 131 (2006) 394–401.